# **Malaysian Journal of Analytical Sciences** (MJAS) Published by Malaysian Analytical Sciences Society



# FORMATION AND STABILITY STUDY OF SILVER NANOPARTICLES REDUCED BY Murdania Loriformis EXTRACT FOR ANTIBACTERIAL APPLICATIONS

(Kajian Pembentukan dan Kestabilan Nanopartikel Perak yang Diturunkan oleh Ekstrak Murdania Loriformis untuk Aplikasi Antibakteria)

Norain Isa<sup>1,2\*</sup>, Nazatul Nabila Mohamad<sup>1</sup>, Ainorkhilah Mahmood<sup>3</sup>, Nor Aziyah Bakhari<sup>3</sup>, Marlina Mohd Mydin<sup>4</sup> and Norhafiza Mohd Arshad<sup>5</sup>

> <sup>1</sup>Chemical Engineering Studies, College of Engineering, Universiti Teknologi MARA, Cawangan Pulau Pinang, Permatang Pauh Campus, 13500 Pulau Pinang, Malaysia <sup>2</sup>Waste Management and Resource Recovery (WeResCue) Group, Chemical Engineering Studies, College of Engineering,

Universiti Teknologi MARA, Cawangan Pulau Pinang, Permatang Pauh Campus, 13500 Pulau Pinang, Malaysia <sup>3</sup>Department of Applied Sciences, Universiti Teknologi MARA, Cawangan Pulau Pinang, Permatang Pauh Campus, 13500 Pulau Pinang, Malaysia <sup>4</sup>Faculty of Health Sciences, Universiti Teknologi MARA,

Cawangan Pulau Pinang Kampus Bertam, 13200 Kepala Batas, Pulau Pinang, Malaysia <sup>5</sup>Centre for Research in Biotechnology for Agriculture, Universiti Malaya, 50603 Kuala Lumpur, Malaysia

\*Corresponding author: norain012@uitm.edu.my

Received: 21 September 2022; Accepted: 30 January 2023; Published: 22 February 2023

#### Abstract

The aggregation of silver nanoparticles (AgNPs) is a serious problem in their applications. This article describes the synthesis of AgNPs using AgNO<sub>3</sub> as a metal precursor and Murdannia loriformis extract (MLE) as a reducing agent. The effect of MLE concentration, AgNO3 concentration, reaction time, and pH on the synthesis of AgNPs was studied using the absorbance of the surface plasmon resonance (SPR) band. From the TEM image, highly scattered AgNPs with a spherical shape and an average particle size of around 12.60 nm ± 2.83 nm were observed for synthesized AgNPs at optimized conditions (pH 8, 100% MLE concentration, 2 mM of AgNO3 and 24 hr reaction time). The stability of synthesized AgNPs was initially studied using a different initial concentration (5 and 10 mM) of the metal precursor. The aggregation process was evaluated by the zeta potential and UV-

# Isa et al.: FORMATION AND STABILITY STUDY OF SILVER NANOPARTICLES REDUCED BY *Murdania Loriformis* EXTRACT FOR ANTIBACTERIAL APPLICATIONS

vis spectra measurements and finally confirmed by TEM. For an antibacterial performance, the disk diffusion method was applied. It was observed that the synthesized AgNPs showed enhanced antibacterial activity depicting the inhibition zone between 18.27 and 22.09 mm reported against *Escherichia coli* (*E. coli*) compared to *Staphylococcus aureus* (*S aureus*), which has an inhibition zone between 9.11 and 10.99 mm. The significance of this study showed that the AgNPs synthesized in this process were found to have efficient antibacterial activity against bacteria *E. coli*. Additionally, the increasing metal precursor concentrations exhibited a reduction in the stability of AgNPs.

Keywords: Murdannia loriformis, silver nanoparticles, stability, Escherichia coli, Staphylococcus aureus

#### **Abstrak**

Penggumpalan nanopartikel perak (AgNPs) adalah masalah serius dalam aplikasinya. Artikel ini menerangkan sintesis AgNPs menggunakan AgNO3 sebagai prekursor logam dan ekstrak *Murdannia loriformis* (MLE) sebagai agen penurunan. Kesan kepekatan MLE, kepekatan AgNO3, masa tindak balas, dan pH ke atas sintesis AgNPs telah dikaji menggunakan penyerapan jalur resonans plasmon permukaan (SPR). Daripada imej TEM, AgNPs yang tersebar adalah dalam bentuk sfera dan saiz zarah purata sekitar 12.60 nm ± 2.83 nm di sintesis pada keadaan optimum (pH 8, 100% kepekatan MLE, 2 mM AgNO3 dan 24 jam masa tindak balas). Kestabilan AgNPs pada mulanya dikaji menggunakan kepekatan awal prekursor logam yang berbeza (5 dan 10 mM). Proses penggumpalan dinilai oleh potensi Zeta dan ukuran spektrum UV/vis dan akhirnya disahkan oleh TEM. Untuk prestasi antibakteria, penyebaran cakera dilaksanakan. Diperhatikan bahawa AgNPs menunjukkan aktiviti antibakteria yang dipertingkatkan yang menggambarkan zon perencatan antara 18.27 dan 22.09 mm yang dilaporkan terhadap *Escherichia coli* (*E. coli*) berbanding *Staphylococcus aureus* (*S aureus*), yang mempunyai zon perencatan antara 9.11 dan 10.99 mm. Kepentingan kajian ini menunjukkan bahawa AgNPs yang disintesis dalam proses ini didapati mempunyai aktiviti antibakteria yang cekap terhadap bakteria *E. coli*. Di samping itu, didapati bahawa peningkatan kepekatan prekursor logam menunjukkan pengurangan kestabilan AgNPs.

Kata kunci: Murdannia loriformis, nanopartikel perak, kestabilan, Escherichia coli, Staphylococcus aureus

### Introduction

This article describes the synthesis, stability and antibacterial study of AgNPs synthesized using AgNO<sub>3</sub> as a metal precursor and Murdannia loriformis extract (MLE) as a reducing agent. Murdannia loriformis (Hassk.) (M. loriformis) is an Indian plant that belongs to the Commelinaceae family. The plant species are found throughout the forests and grassy slopes of Asia, especially in China and Thailand [1]. This plant is gaining popularity in Malaysia due to its therapeutic potential for conditions such as psoriasis and dermatitis [2]. M. loriformis is one of Thailand's most popular folk medicines for cancer and diabetes patients. It is thought to slow cancer progression as well as provide symptomatic relief from contemporary therapy [3]. M. loriformis is also a traditional Chinese remedy for detoxifying respiratory tract problems [4]. M. loriformis is known as "Beijing grass," or "Angel grass" in English, "Rumput Cina," "Rumput Beijing," and Rumput Siti Khatijah in Malay and "Ya Pak King" in Thailand (Figure 1). The phytochemical analysis of M. loriformis found that the plant's extract contains phenolics, flavonoids, condensed tannin, carbohydrates,

protein, and plant membrane lipids [2, 5, 6]. Several scientific reports support the traditional use of *M. loriformis* in treating different ailments. From the kinds of literature, *M. loriformis* extract possesses numerous pharmacological properties, including antioxidant, antimutagenicity, anticancer, anti-inflammatory, immunomodulatory effects, antipyretic, analgesic, antimicrobial, antibacterial, and gastroprotective activity, which support its traditional use [2]. Due to the phytochemicals and properties of *M. loriformis*, this plant is selected as a potential reducing agent for synthesis of AgNPs.

The scientific world has recently given special attention to the use of bioresources in nanotechnology due to their eco-friendly properties, availability, and low cost, and *M. loriformis* has a promising future in this regard [7]. Nanomaterials have piqued the interest of the scientific community due to their unique properties and diverse biomedical and environmental remediation applications [7–11]. Nanomaterials, such as silver nanoparticles (AgNPs), have numerous possible applications, such as medical diagnostics, imaging, medication delivery,

identification of biological samples, solar cells, catalysis, photovoltaics, and digital data storage [12]. The most famous application of AgNPs is their usage in environmental cleaning. Due to the use of benign phytochemicals and the elimination of dangerous molecules that would have been employed in chemical synthesis, the green synthesis of nanoparticles has earned considerable favor [13]. This technique utilizes bio-extracts as reducing agents, making them relatively less expensive, quicker, and easier than alternative processes. Controlling the size, shape, and structure of AgNPs is crucial due to the close correlation between these features and their optical, electrical, and catalytic properties [14].



Figure 1. Murdannia loriformis plant

In this study, AgNPs were synthesized using silver nitrate as a metal precursor and *Murdannia loriformis* extract (MLE) as a reducing agent. The stability of synthesized AgNPs was investigated and characterized by a variety of characterization techniques. Then, the antibacterial properties were studied against *Escherichia coli* (*E. coli*) and *Staphylococcus aureus* (*S. aureus*) using the disc diffusion method.

#### **Materials and Methods**

#### Materials

Silver nitrate, 99.8%, and sodium hydroxide, 99%, were purchased from QReC. Sulphuric acid, 95-97%, was acquired from Supelco. The aerial part of *Murdannia loriformis* was acquired from EES Biotech Sdn Bhd, Penang, then dried and ground into a fine powder. The powder was then added to 200 mL of deionized water in a 250 mL beaker and heated at 70 °C for 1 hour. Using Whatman No. 1 filter paper, the extracts were filtered

and stored at 4 °C for future use. This solution was considered as 100% *Murdannia loriformis* extract (MLE). The *Escherichia coli* ATCC 25922 PK/5 and *Staphylococcus aureus* subsp. aureus ATCC 29213 PK/5 were purchased from Oxoid. The chemicals were used without further purification.

#### Identification of phytoconstituent in MLE

The phytochemical screening test was conducted using standard procedures Sofowora, 1993; Trease and Evans, 1989; Harborne, 1973 to identify the chemical compounds in the MLE [15]. Table 1 summarizes the experimental for the selected screening test for this study. Carbohydrates content was determined using the calculation method suggested by Guide to Nutrition Labelling and Claims (2010) [16]. The protein content was determined using the Kjeldahl method, protein content was determined as  $N \times 6.25$ . The average nitrogen (N) content of proteins was found to be about 16 percent, which led to the use of the calculation N x 6.25 (1/0.16 = 6.25) to convert nitrogen content into protein content. The functional group in compounds was determined using a Nicolet FTIR spectrophotometer (Thermoscientific Nicolet 6700, USA). A small amount of powdered Murdannia loriformis was respectively placed directly on the germanium piece of the infrared spectrometer with constant pressure applied, and data of infrared absorbance, collected over the wave number ranged from 500 to 4000 cm<sup>-1</sup> and computerized for analyses by using the Omnic software (version 5.2). The reference spectra were acquired from the cleaned blank crystal prior to the presentation of each sample replicate.

#### Synthesis of AgNPs: Effect of Variable Parameters

The preparation of AgNPs was observed by the appearance of the characteristic of surface plasmon resonance (SPR) due to the combined vibration of free electrons of AgNPs in resonance with the light wave. The optimization studies were carried out for the formation AgNPs in order to find the optimized condition using MLE as a reducing agent and AgNO<sub>3</sub> as the metal precursor. As to ensure the results of the experiments were run in triplicates. The formation of AgNPs at different pH, MLE concentrations, AgNO<sub>3</sub> concentration, temperature, and reaction time were analyzed using a

UV-Vis spectrophotometer.

Table 1. Screening test for identification of phytochemicals in MLE

Test	Experimental	Explanation	
Tannin	About 0.5 g of the dried powdered samples were	Brownish green	
	boiled in 20 ml of water in a test tube and then	or a blue-black colouration indicates the	
	filtered. A few drops of 0.1% ferric chloride	presence of tannins.	
	were added.		
Flavonoids	NaOH (2 mL, 10%) was added to MLE, and the	The yellowish colour will turn colourless if	
	solution turned to yellowish colour. Dilute HCl	flavonoids are present.	
	was added to the mixture.		
Saponins	A small portion of the crude sample was	A layer of foam (around 1 cm) is formed if	
	dissolved in 1 mL of ethanol and then diluted	saponins are present in the mixture.	
	with distilled water. The mixture was placed in		
	a shaker for 15 minutes.		
Sterols	Chloroform solution of the extract when shaken	The red colour of the solution indicates the	
	with concentrated sulphuric acid.	presence of sterols.	
Terpenoids	This test is known as the Salkowski test.	A reddish-brown layer formed on the	
	Chloroform (2 mL) was added to 5 mL of MLE.	surface of the mixture indicates the	
	Then, 3 mL of concentrated H <sub>2</sub> SO <sub>4</sub> was added	presence of terpenoids.	
	carefully into the mixture.		

# Effect of pH

The effect of pH on the synthesis of AgNPs was studied. At this stage, 1 mL of 2 mM of AgNO<sub>3</sub> as the metal precursor and 9 mL of 100% MLE as reductant were kept constant. The pH of the solution was adjusted to pH 2, 4, 6, 8, and 10 using 0.1 M of NaOH and H<sub>2</sub>SO<sub>4</sub>, respectively.

### Effect of AgNO3 as metal precursor

The effect of metal precursor concentration on the synthesis of AgNPs was examined using 1 mL of varied AgNO<sub>3</sub> concentrations from 1 mM to 15 mM. In this part, 9 mL of 100% MLE was used as a reductant at constant pH 8 and room temperature.

#### Effect of contact time

The effect of contact time on the synthesis of AgNPs was set at different time intervals, which were 20, 40, and 60 min. In this experiment, 1 mL of 2 mM of AgNO<sub>3</sub> as a metal precursor, 9 mL of 100% MLE as a reductant, and pH 8 were kept constant.

#### Effect of MLE concentration as reductant

In order to optimize the amount of extract as a reductant for the synthesis of AgNPs, 100% MLE concentration (10 g in 200 mL solution) was prepared, and the solution was diluted to 25, 50, and 75%, respectively. In this experiment, 1 mL of 2 mM of AgNO<sub>3</sub> as a metal precursor and 9 mL of reductant was kept constant at pH 8.

## **Characterization of AgNPs**

Characterization of AgNPs was carried out using various characterization techniques. Information about optical properties, surface, morphology, particle size, shape, crystal structure, and chemical composition related to the sample was unveiled.

The optical characteristics of the samples were determined using Lambda 35 Perkin Elmer UV-vis spectroscopy with a 10 mm quartz sample cuvette optical path length. The synthesized AgNPs were placed in a sample cuvette and then scanned in a sample chamber. The range of the scan was 400 to 800 nm. The increase in the relative intensity of the SPR peaks

indicates a growing concentration of AgNPs in the system. The shape, size, and average size distribution were determined utilizing Phillips CM12 TEM with Docu version 3.2 image processing, High-Resolution Transmission Electron Microscope (HRTEM) 200 kV with Field Emission TECNAI G20S-TWIN, FEI, and Malvern Zetasizer, respectively. By enabling a highenergy electron to pass through the sample during the TEM measurement, an image with atomic resolution is the meantime, produced. In HRTEM crystallographic information about samples by measuring the interplanar spacing (d-spacing) and grain boundaries with atomic resolution.

The X-ray diffraction (XRD) investigation was carried out using a Philips FW1710 and Cu K radiation. The development of diffraction patterns is analysed and identified by comparing the diffracted beams to the reference database stored in the International Centre for Diffraction Data (ICDD) library. The diffracted patterns reveal whether the sample materials are pure or contaminated. Thermo Scientific (Nicolet 6700) FTIR spectrometer was used to analyse functional groups that exist in AgNPs in the range of 500-4000 cm<sup>-1</sup>. FTIR spectroscopy is used to determine whether biomolecules in MLE are involved in AgNP production.

The criteria of stability of AgNPs are measured when the values of zeta potential range from higher than +30 mV to lower than -30 mV. Surface zeta potentials were measured using the laser zeta meter (Zeta Sizer- Nano Zs). Colloidal AgNPs (5 mL) was diluted with double distilled water (50 mL) using NaCl as suspending electrolyte solution (2 x10<sup>-2</sup> M NaCl). The pH was then adjusted to the required value. The samples were shaken for 30 minutes. After shaking, the equilibrium pH was recorded, and the zeta potential of the AgNPs was measured. A zeta potential was used to determine the surface potential of the AgNPs. The chemical composition of the samples has been obtained with EDX using a Hitachi S3700N SEM instrument equipped with a Bruker Quantax EDX system.

The preparation of AgNPs was observed by the appearance of the characteristic of surface plasmon resonance (SPR) due to the combined vibration of free

electrons of AgNPs in resonance with the light wave. The formation of AgNPs at different AgNO<sub>3</sub> concentrations from 1 mM to 15 mM was analyzed using a UV-Vis spectrophotometer. To study the stability of synthesized AgNPs, the formation of AgNPs was further investigated using 2, 5, and 10 mM of initial concentration of metal precursor at longer reaction time (1 week and 1 month) and characterized using UV-vis, TEM, and Zeta potential.

#### **Antibacterial test**

The production of fresh germs is required for antimicrobial experimentation. Fresh culture is used to cultivate microorganisms that were present 24 hours prior. The linear culture was employed to create a new culture. A single colony was extracted from the cultures and dissolved in the culture's nutrient broth after the loop had been sterilized by heat and cooled. After the culture medium containing the bacteria had been transferred, the tubes holding the normal saline were thoroughly mixed with a vortex for 24 hours until the suspension turbidity was equal to 0.5 McFarland. This opacity is equal to 1.5 x 108 CFU/mL. Two bacterial species, namely E. coli (ATCC No. 25922) (EC) and S. aureus (ATCC No. 29213) (SA), were procured from Next Gene Scientific Sdn. Bhd as Culti-loops. Each bacterial strain was activated on Mueller Hilton Agar, constant at 37 °C for 18 hours. Then 30  $\mu L$  of the broth was transferred to nutrient agar and incubated at 37 °C for another 24 hours; cell concentration was 10<sup>8</sup> cfu/mL. The effects of antibacterial were studied using the disc diffusion technique. The microbiological suspension of single-colonies of bacteria was generated in accordance with the standard at 0.5 McFarland's to study the antibacterial impact of the disc diffusion technique. On agar nutrition, several bacteria were cultivated independently. 10 mL of different concentrations of AgNPs (2, 5, and 10 mM) and negative controls (MLE) were put onto the disc using the sampler. The plates were then incubated in an oven set to 37°C. Additionally, there was no microbial cloud formation after 24 hours.

# **Results and Discussion**

Three approaches were used to identify phytoconstituents in MLE: phytochemical screening

and carbohydrate and protein content testing. To identify the chemical components found in the MLE, a phytochemical screening test was performed. Table 2

displays the phytochemical screening results, which revealed the presence of flavonoids and sterols but no alkaloids, terpenoids, or saponins.

Chemical Compound	Presence Description		
Alkaloids		Alkaloids are absent	
Terpenoids		Terpenoids are absent	
Flavonoids	++	Flavonoids are present	
Saponins		Saponins are absent	
Sterols	++	Sterols are present	

Carbohydrates content was determined using the calculation method suggested by Guide to Nutrition Labelling and Claims (2010) [16]. The protein content was determined using the Kjeldahl method. The total carbohydrates and protein content in the MLE were found to be 67.20% and 8.90%, respectively. FTIR spectroscopic analysis was then applied to characterize MLE and the synthesized MLE-mediated AgNPs

(Figure 2). The FTIR spectrum of AgNPs showed a strong peak at 3257-3371 cm<sup>-1</sup>, which is a characteristic of the -OH stretching modes in the hydroxyl functional groups. Distinct peaks at 1632-1638 cm<sup>-1</sup> were observed, in which the second peak is related to the hydroxyl functional groups of alcohols and phenolic compounds that might exist in MLE.

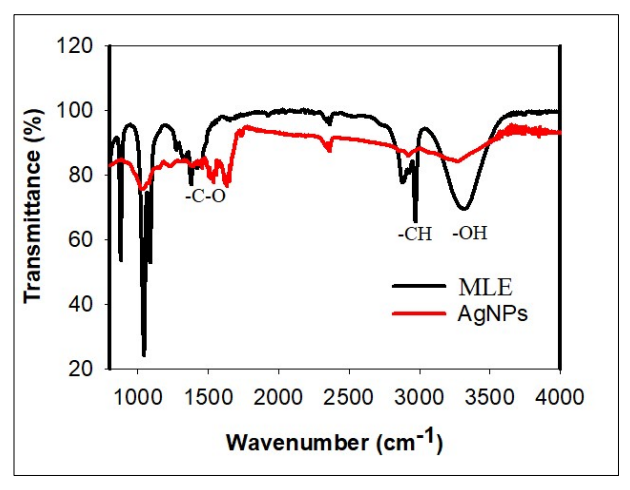


Figure 2. FTIR spectra for MLE and MLE-mediated AgNPs

The distinct band within 1632-1645 cm<sup>-1</sup> could be linked to the aromatic compounds of carbon and carbon double bonds. The sharp band at 1032-1051 cm<sup>-1</sup> indicates the presence of the -C-O group, and the absorption bands at 1714-1732 and 1635-1655 cm<sup>-1</sup> correspond to the presence of the carbonyl group within the extract. The observed peaks in the range of 1075-1079 cm<sup>-1</sup> can be related to the combination of alcohols and phenols. The band at 2923 - 2913 cm<sup>-1</sup> indicates -CH stretching

vibrations. Most of the absorption bands that appeared in the IR spectrum of the aqueous MLE could also be observed in the IR spectra of synthesized AgNPs. This shows that the phytoconstituents biomolecules protect the AgNPs from aggregation. The synthesis of AgNPs by MLE as source of biomolecules was done by some metabolite's functional groups such as alcohols. Similar findings have also been reported in other studies [17].

### Synthesis of AgNPs: Optimization studies

AgNPs were formed as a result of the reduction of Ag<sup>+</sup> by MLE. The presence of a band indicative of Surface Plasmon Resonance (SPR) around 410-455 nm validated the development of AgNPs. The AgNPs have free electrons, which cause the SPR absorption band to form as a result of the coupled vibration of AgNPs' free electrons in resonance with light waves. Reaction time, pH, precursor concentration, MLE concentration, and temperature were among the synthesis parameters studied. The findings are organized under the following headings.

# Effect of pH

The influence of pH on the formation of AgNPs has been investigated using a pH range of 2-10 and was plotted in Figure 3(a). From Figure 3(b), it can be seen that the

intensity of the SPR peak increases when it increases pH from pH 2 to pH 10. In view of the results obtained, the formation of AgNPs is favourable under basic conditions. The addition of NaOH does not bring negative consequences on the formation of AgNPs. Alas, the SPR peak of synthesized AgNPs is higher than in acidic form. However, with the addition of acid solution, the SPR peaks show lower and broader absorbance compared to pH 8 and 10. It can be observed that the SPR peaks for acidic conditions (pH 2) appear at a relatively short wavelength of around 401 nm, while the SPR peaks are shifted towards a longer wavelength (red shift) at 423 nm in the case of the basic medium as shown in Figure 3 (c). The red shift in a basic medium indicates relatively large AgNPs sizes compared with the cases of neutral and very acidic conditions (pH 2).

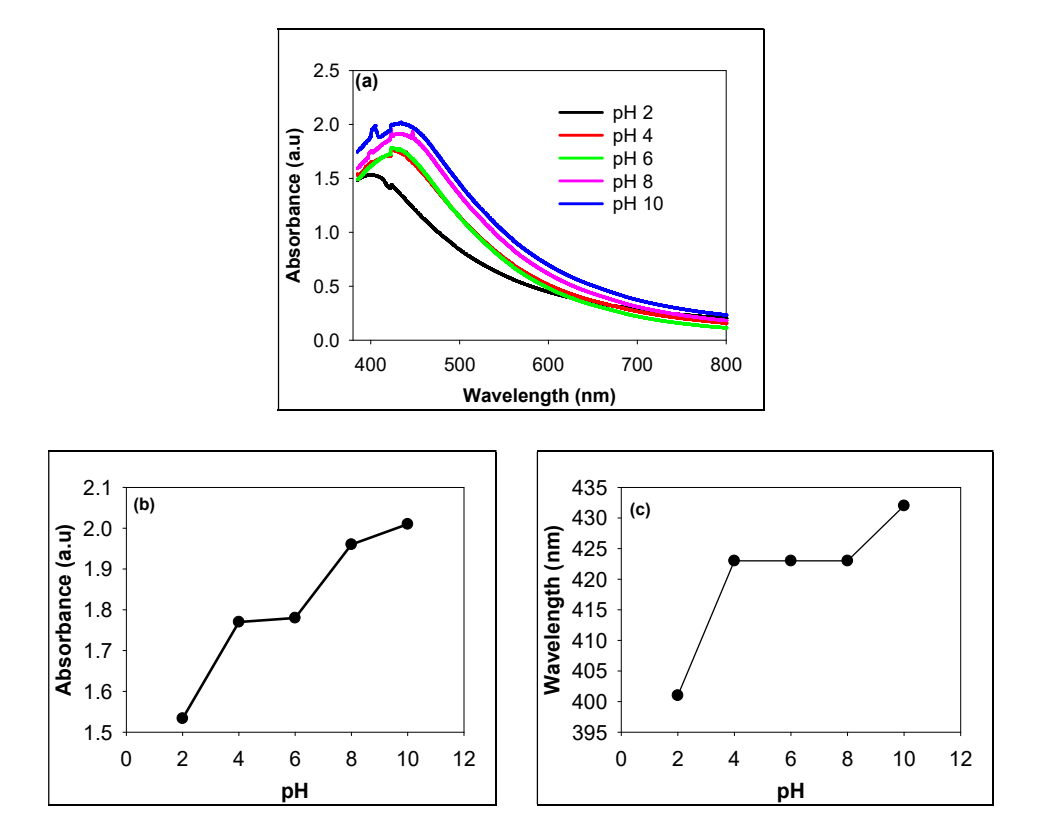


Figure 3. Effect of pH on SPR peak of synthesized AgNPs

#### Effect of concentration of MLE

Figure 4(a) shows the SPR peak for the effect of MLE concentration as a reducing agent in the formation of

synthesized AgNPs. As seen in Figure 4(b), the intensity of SPR peak at 423 nm increases when the initial concentration of MLE increases from 25% to 100%. The

increases in SPR peak with increasing concentrations of MLE can be explained by the increase in the amount of active ingredient in a higher concentration of MLE. At low concentrations of MLE (25% and 50%), the

synthesized AgNPs do not have enough reducing agents for synthesizing AgNPs and fail to stabilize the high surface energy of AgNPs. Similar findings have also been reported in other studies [10].

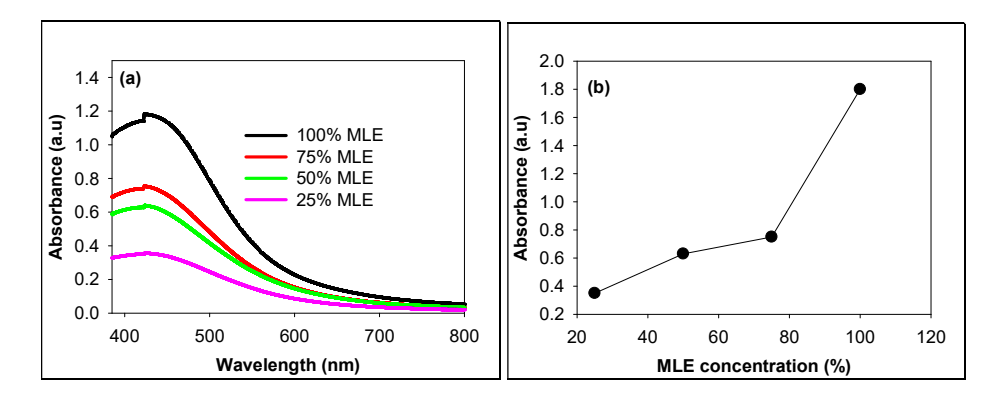


Figure 4. Effect of MLE concentration on SPR peak of synthesized AgNPs

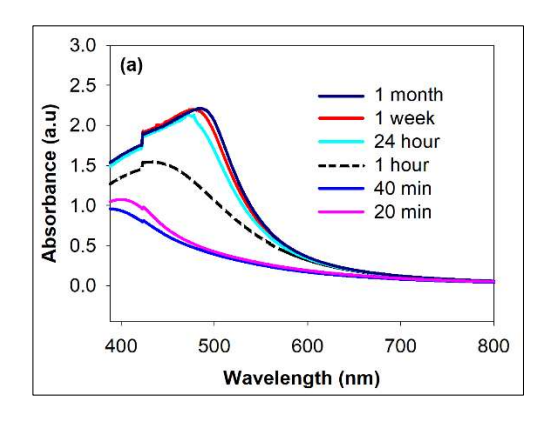
#### Effect of reaction time

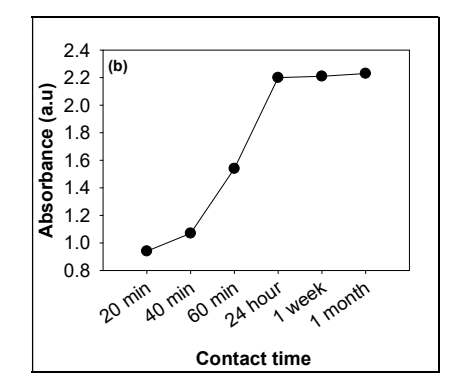
The effect of reaction time on the SPR peak of synthesized AgNPs is shown in Figure 5(a). The intensity of the SPR peak increases with increasing the reaction time from 20 mins to 60 mins, as shown in Figure 5(b). It was noted that with an increase in contact time, the SPR peak becomes sharper. Formation of AgNPs started within 20 mins and increased up to 60 mins. For the stability study, the SPR peak was evaluated for 24-hour, 1-week, and 1-month contact time, as shown in the same spectra in Figure 5(a). However, the SPR peaks in Figure 5 (b) show higher and sharper absorbance compared to the initial reaction time (20-60 mins). It can be observed that the SPR peaks are shifted towards a longer wavelength (red shift) at 479 nm - 482 nm, as shown in Figure 5(c). The redshift at longer contact times indicates relatively larger size AgNPs were obtained. This is due to unstable AgNPs produced and cause agglomeration after a longer contact

time.

#### Effect of concentration silver nitrate

Figure 6 (a) shows the SPR peak for the effect of different concentrations of silver nitrate as a metal precursor from 1 to 15 mM at 1 h reaction time. It can be seen that the intensity of the SPR peak of synthesized AgNPs appears to increase with increasing silver nitrate concentration until it reaches a maximum SPR peak at 430 nm for 5 mM, as shown in Figure 6 (b) – (c). However, the after the SPR peak decreased for higher concentration. No significant SPR peak for 1, 2, and 4 mM of silver nitrate, indicating that low concentrations of Ag<sup>+</sup> are not enough to induce the formation of AgNPs. For 10 mM and 15 mM silver nitrate concentration, the SPR peaks decreased with increasing silver nitrate concentration due to the agglomeration of AgNPs at high concentrations of the metal precursor.





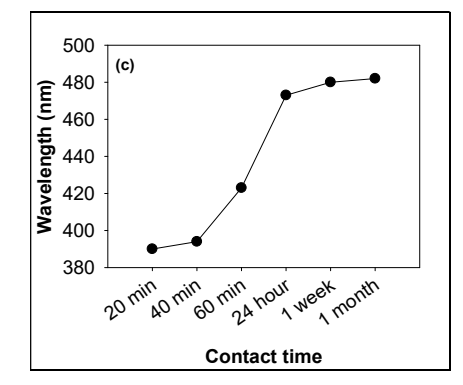


Figure 5. Effect of contact time

# **Characterization of AgNPs**

AgNPs were synthesized at selected parameters, and the optimum condition was further characterized to evaluate their features, such as size, shape, crystallinity, morphology, form, elemental composition, and surface chemistry.

#### Transmission electron microscopic (TEM) analysis

Figure 7(a-c) show the TEM, HRTEM, and size distribution (histogram) of synthesized AgNPs, respectively. From Figure 7(a), the shape of the colloidal AgNPs was quasi-spherical, and the particles were observed to be evenly distributed. Figure 7(b) shows the HRTEM image of a single AgNP; from the HRTEM, it can also be seen that AgNPs are capped with the

phytoconstituents, which is likely to be MLE as a reducing as well as capping agent. The lattice spacing of 0.23 nm was calculated for the HRTEM of a single AgNP, which is associated with (111) plane of AgNPs and with a diameter of 16.16 nm. This indicates the success in the use of MLE not only as a reductant, as it was intended but also as a capping agent to avoid agglomeration of the particles. From Figure 7 (c), the range of particle size of the AgNPs, as calculated from the histogram, was between 8.25 and 19.34 nm with an average particle size of 12.60 nm  $\pm$  2.83 nm. Similar findings have also been reported in other studies about the plant extract capped the AgNPs [17, 18].

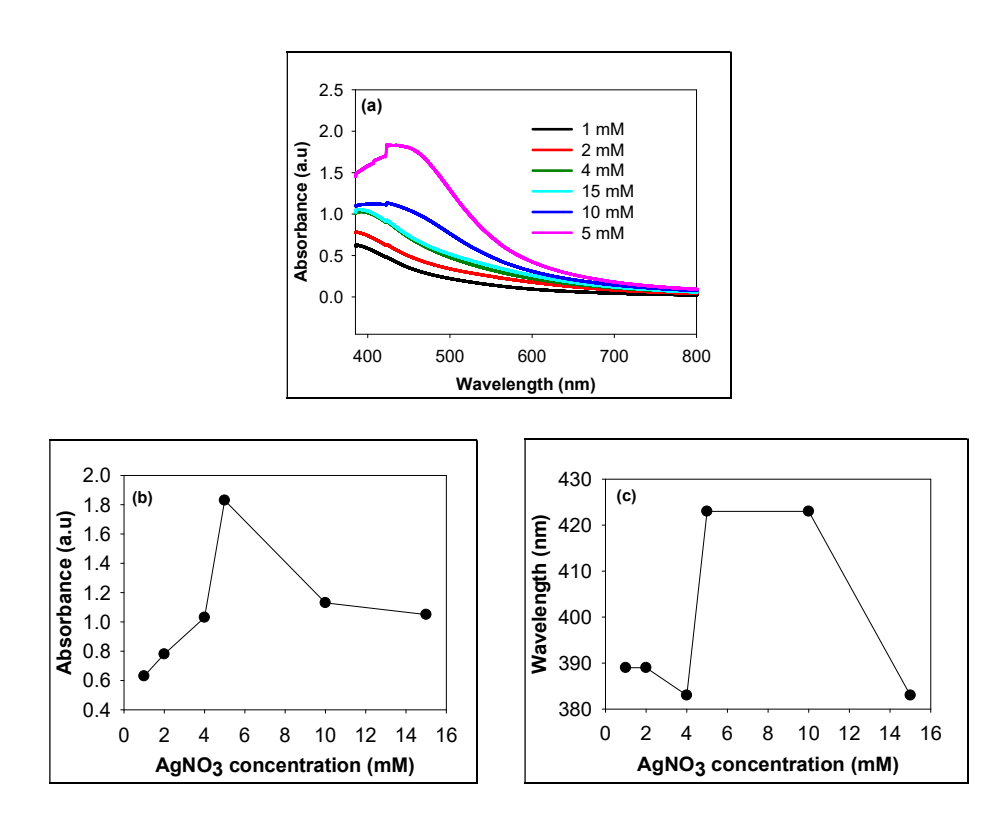


Figure 6. Effect of concentration of metal precursor

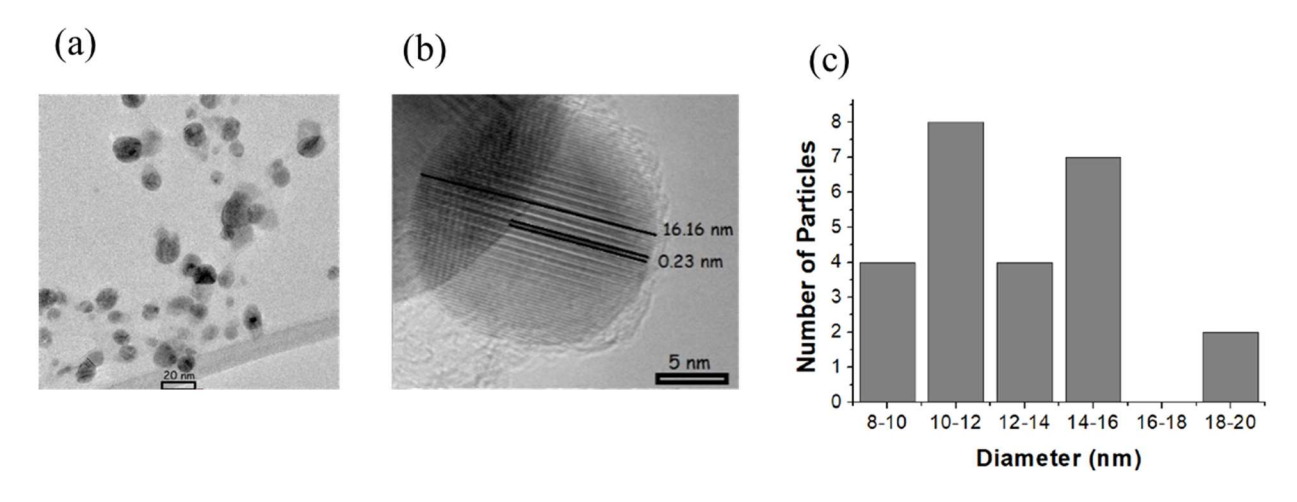


Figure 7. (a) TEM image, (b) HRTEM, and (c) histogram for the size distribution of 2 mM MLE-mediated AgNPs

# The crystallinity of Synthesized AgNPs

Figure 8 shows the XRD pattern that proved the crystallinity of the synthesized AgNPs. The freeze-dried MLE-mediated AgNPs' XRD peaks matched the FCC structure of silver at 2 of 38.08°, 44.16°, 64.40°, and

76.85°, corresponding to the (111), (200), (220), and (311) planes, respectively. The (111) plane is found to be more intense than other planes, indicating that growth is concentrated along the (111) plane. The same pattern was also reported in other studies [19, 20].

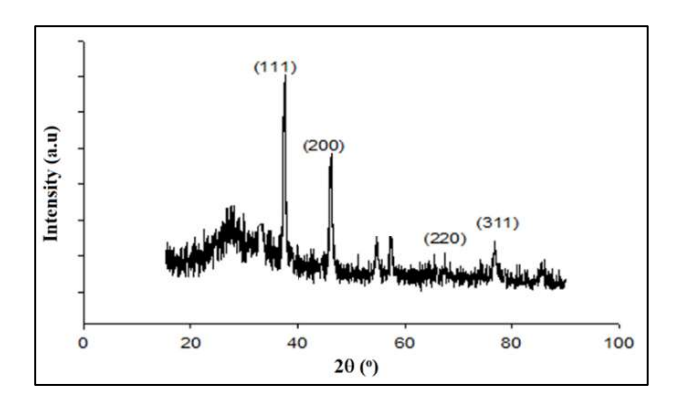


Figure 8. XRD pattern for MLE-mediated AgNPs

#### Particle size distribution and zeta potential

The Malvern Zetasizer was used to determine the particle size distribution and the zeta potential. Figure 9(a) depicts the hydrodynamic diameter size for synthesized AgNPs prepared using a different initial concentration of metal precursor of 1, 2, 5, and 10 mM. From

Figure 9(a), it can be seen that the smallest hydrodynamic diameter size of 55.25 nm for synthesized AgNPs prepared at 5 mM and the biggest size of 86.09 nm at 2 mM of initial metal precursor concentration. The increases in the hydrodynamic size of synthesized AgNPs at 2 mM initial concentration might be explained by the optimum amount of the active ingredient in MLE reacted with metal precursor at 2 mM. However, with the increasing initial concentration of metal precursor to 5 mM and 10 mM, the amount of active ingredient is not enough to reduce and stabilize the synthesized AgNPs at high concentrations.

The results obtained were supported by the zeta potential value of synthesized AgNPs at a different initial concentration, as shown in

Figure 9(b). The results showed that synthesized AgNPs prepared using 2 mM have the highest zeta potential value of 23.61 mV. The high potential value could be attributed to the capping action of MLE phytoconstituents, resulting in well-dispersed synthesized AgNPs at 2 mM concentration. The zeta potential for 5 mM and 10 mM of synthesized AgNPs was decreased to 15.80 and 9.75 mV, respectively. It is known that colloids with high zeta potential (negative or positive) are electrically stable, while colloids with low zeta potential tend to coagulate or flocculate [11].

The PDI of the synthesized AgNPs (Figure 9(c)) was in the range between 0.27 and 0.40, showing that the are synthesized **AgNPs** monodispersed monodispersed systems, the PDI should be 0.01 - 0.7 [14]. Colloids with a high zeta potential (negative or positive) are electrically stable, whereas colloids with a low zeta potential coagulate or flocculate [21]. The difference in size between HRTEM and particle sizer measurements could be attributed to the particle sizer assessing the hydrodynamic size of the AgNPs (size of the dispersed AgNPs solvated along with the phytoconstituents of MLE as capping and stabilizing agents).

Figure (d) shows the particle size analysis for synthesized AgNPs prepared at an concentration of 2 mM of initial metal precursor concentration. The particle size analyzer detected two particle size ranges (1-10 nm and 10 - >100 nm). This finding implies that the AgNPs produced are polydispersed particles. Smaller particles (1-10 nm) have a lower peak intensity, whereas larger particles (10 -100) have a greater intensity with a Z-average of 86.09 nm. Small particles may arise in the proximity of larger ones. According to Yin et al., small particles surrounding large particles are most likely generated via second-round nucleation. The larger AgNPs were produced by accelerated crystal development, but their varied sizes of AgNPs may occur due to their formation at different times [22].

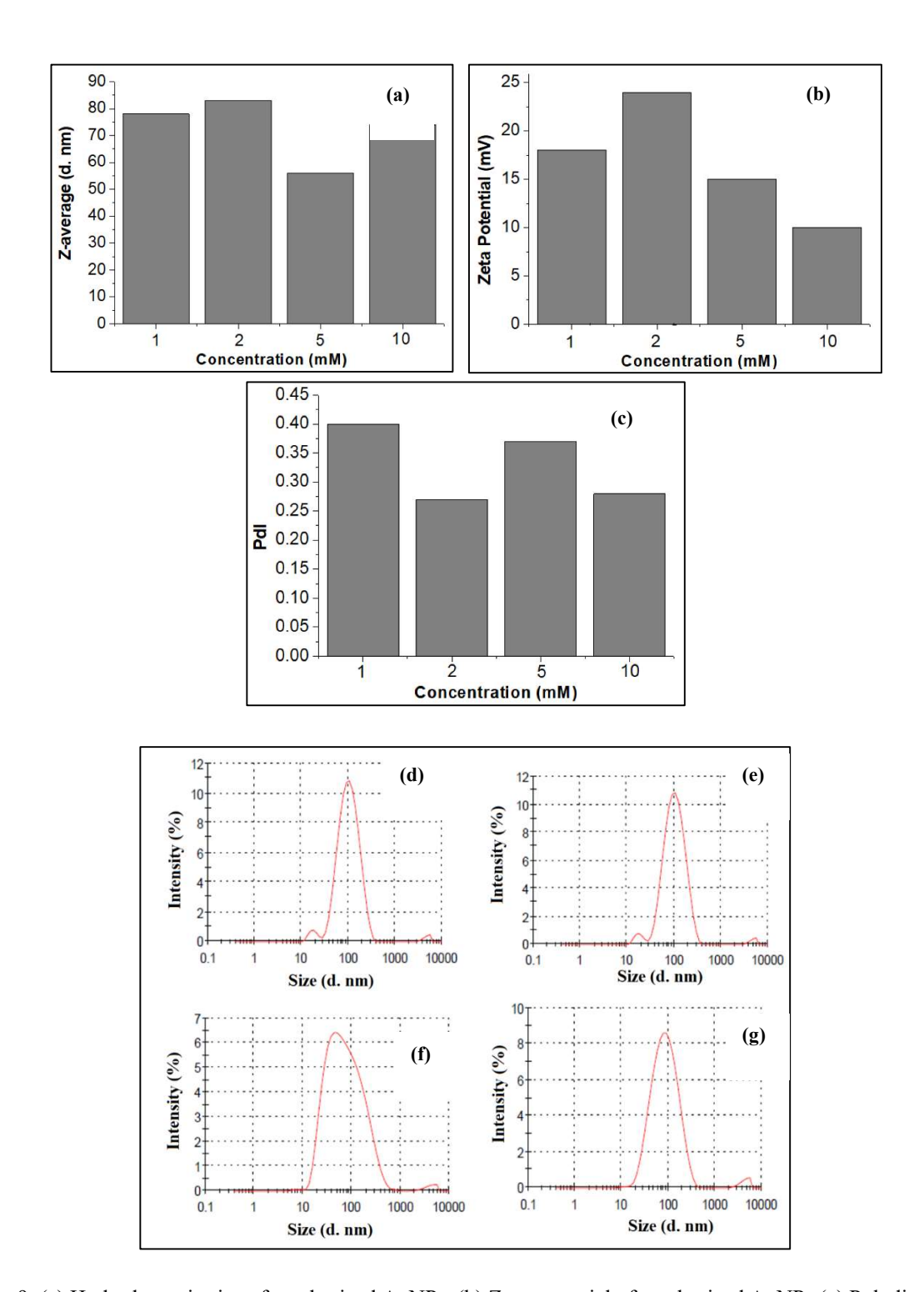


Figure 9. (a) Hydrodynamic size of synthesized AgNPs (b) Zeta potential of synthesized AgNPs (c) Polydispersity index of synthesized AgNPs. Particle size analysis of synthesized AgNPs at (d) 1 mM, (e) 2 mM, (f) 5 mM, and (g) 10 mM initial concentration

### Chemical composition analysis

The chemical composition of the synthesized AgNPs was determined by energy-dispersive X-ray spectroscopy (EDX), as shown in Figure 10. It can be

seen that the EDX spectrum consisted of Ag, C, O, and Cl. The EDX data of synthesized AgNPs shows a peak at around 2.6 keV; another intense peak appears at 3 keV for silver (42.20 wt%).

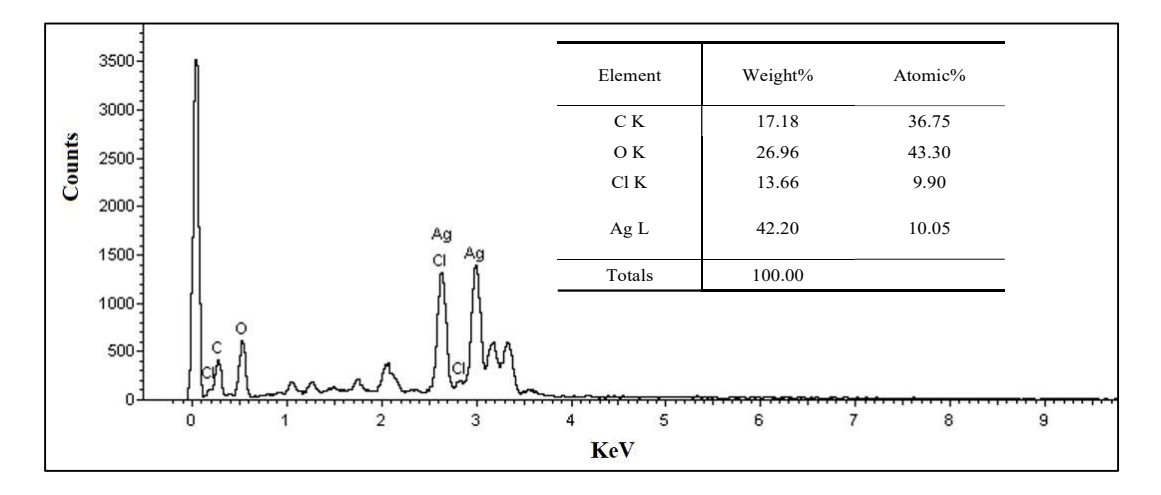


Figure 10. EDX of synthesized AgNPs

# Stability study of AgNPs

After 24 hours, the AgNPs' stability was checked. The synthesized AgNPs created using 2 mM AgNO<sub>3</sub> as the metal precursor was shown to be as stable as when they were originally formed. This is seen in Figure 11(a). Even after a 24 h reaction period, the colour of the colloidal AgNPs solution changed from pale yellow to dark brown without any sedimentation. It was thought that the phytoconstituents in the MLE were effective in giving the MLE-mediated AgNPs stability. AgNPs are coated by the phytoconstituents in MLE, which prevents aggregation and provides stability for a while. MLE

have large concentrations of protein and carbohydrates, which may be what prevents AgNPs that are mediated by MLE from agglomerating.

However, when the concentration of metal precursor increased to 5 mM and 10 mM, the stability of AgNPs decreased significantly, as shown in Figure 11 (b-c). The color of the solution was dark brown, but after 24 h, the precipitation of AgNPs occurred due to the instability of the MLE-mediated AgNPs. Agglomeration of AgNPs shows the larger size of nanoparticles.

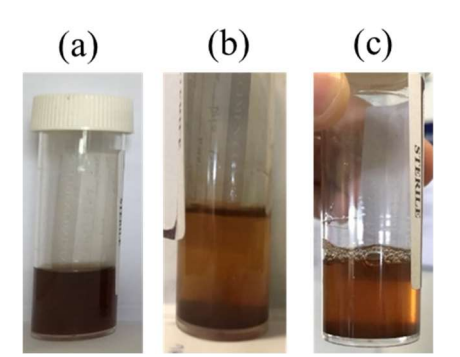


Figure 11. Colour changes of MLE-mediated AgNPs at different concentrations of silver nitrate as metal precursor; (a) 2 mM, (b) 5 mM, and (c) 10 mM

The TEM images were displayed in Figure 12(a) through (c) at various concentrations. Using 5 and 10 mM of AgNO<sub>3</sub> as the metal precursor, the synthesized

AgNPs are clearly shown from the TEM pictures that the particles of AgNPs are agglomerated and form larger particles at high concentrations.

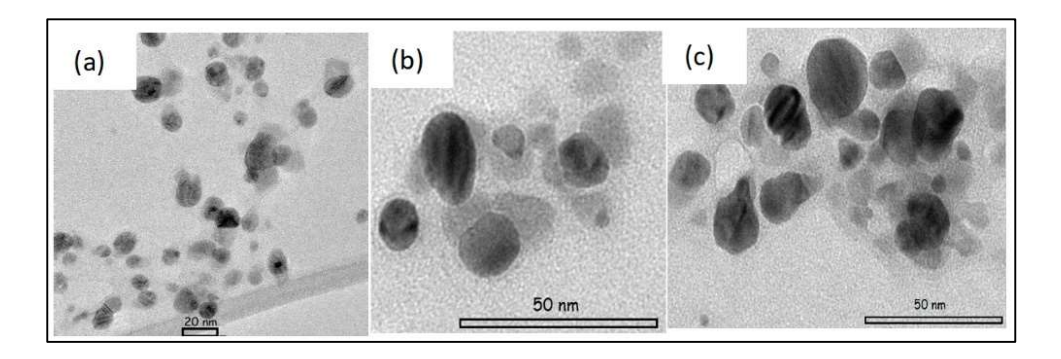


Figure 12. TEM images of MLE-mediated AgNPs at different concentrations; (a) 2 mM, (b) 5 mM, and (c) 10 mM

Figure 13 shows the SPR peak for different concentrations of silver nitrate as a metal precursor (2 mM, 5 mM, and 10 mM) after 24 h reaction time. It can be seen that the intensity of the SPR peak of AgNPs using 2 mM of AgNO<sub>3</sub> is higher than SPR for 5 mM and

10 mM concentrations. It also clearly showed the red shift in peak values from 439 nm to 434 nm and 396 nm for 5 mM and 10 mM, respectively. The red shift of the SPR peak indicated the formation of larger AgNPs.

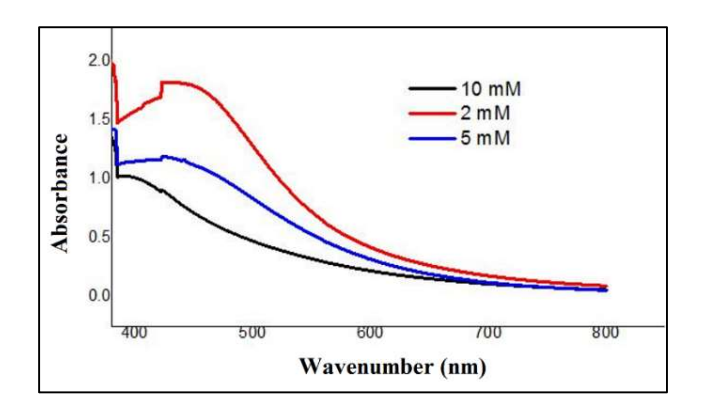


Figure 13. SPR peak from UV-vis of AgNPs at different concentrations after 24 hours

Zeta potential is a useful tool for predicting the stability of AgNPs in solution and understanding their surface. Zeta potential measurement is a technique for determining the surface charge of NPs in a colloidal solution. Figure 14 shows the Zeta potential of AgNPs at different concentrations (2, 5, and 10 mM). From the zeta potential value, it showed that the stability of AgNPs at high concentrations suffers from stability.

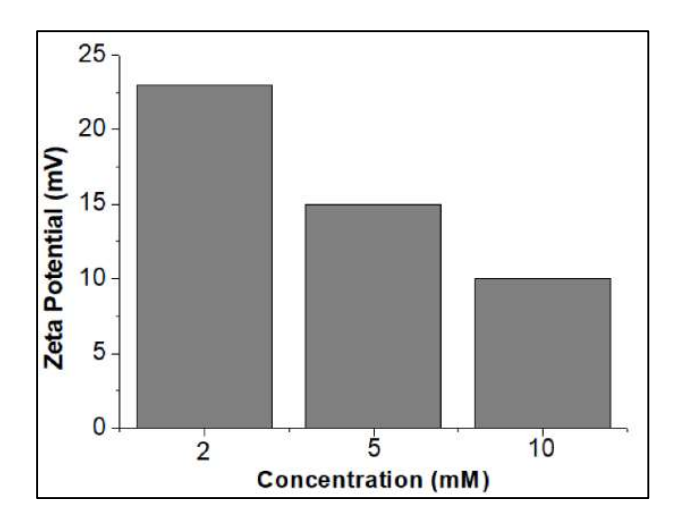


Figure 14. Zeta potential of AgNPs at different concentrations after 24 hours

This section's conclusion clearly shows that using 5 and 10 mM of AgNO<sub>3</sub> lowered the stability of synthesized AgNPs. Adopting the idea demonstrated the size distribution's heterogeneous nature [24]. Additionally, it might be because the biomolecules in the MLE were insufficiently powerful to maintain the high concentration of AgNPs. The production of precipitation for AgNPs created by increasing the concentration of metal precursor was also demonstrated in earlier research [25, 26].

According to the data above, the stability of AgNPs produced by MLE reduced as metal precursor concentration increased. AgNPs must be prepared as a homogeneous mixture with various organic, inorganic, and polymeric components for the majority of real-world applications. To study the impact of polymer on the stability and toxicity of high concentrations of AgNPs, two different polymers were evaluated as stabilizing agents for high concentrations of AgNPs (5 mM and 10 mM).

# Antibacterial studies of AgNPs

The antibacterial efficacy of synthesized AgNPs was tested against Gram-positive (*Staphylococcus aureus*) and Gram-negative (*Escherichia coli*) pathogens. Each pathogen strain was purchased from Next Gene Scientific Sdn Bhd. Antimicrobial tests were then conducted according to the American Society for Testing and Materials (ASTM) standard method E2783-

Biosynthesized AgNPs showed significant antimicrobial activity against both the pathogenic bacteria, i.e., E. coli and S. aureus. The mean diameter of the inhibitory zone (mm) around each well was measured and tabulated in Table 3 result shows Murdannia loriformis extract didn't exhibit any significant antibacterial activity against test pathogens even at high concentrations, which might be due to the active constituents responsible for the antibacterial activity is not present in aqueous leaf extract, or the concentrations are very low. E. coli (Gram-negative bacteria) and S. aureus (Gram-positive bacteria) were sensitive to synthesized AgNPs. The most sensitive is E. coli, around 18.27-22.09 mm, while S. aureus, around 9.95-10.99 mm in diameter, is related to concentration bacteria 30 µL. It was also observed that the maximum of inhibition increases with increasing concentration of AgNPs, where E. coli (Gram-negative) exhibited a higher zone of inhibition as compared to S. aureus (Gram-positive) (Figure 15). From the observation, different concentrations of MLE-mediated AgNPs did not bring much difference in antibacterial properties against both bacteria.

This might be due to the rigid peptidoglycan layer on the Gram-positive bacterial cell wall compared to Gramnegative bacteria preventing the AgNPs from penetrating, resulting lower zone of inhibition. The exact mechanism behind the antibacterial activity of AgNPs is not very clear, but many proposals have been

put forward for the same. The most accepted hypothesis are i) the formation of pits on the outer membrane progressively release the lipopolysaccharides and membrane proteins, ii) cells treated with AgNPs lead to increase conductivity resulting in leakage of the

intracellular molecules, and iii) AgNPs interrupts the ATP metabolism and DNA replication preferentially by targeting the sulfur and phosphorous rich macromolecules resulting programmed cell death.

Table 3 Antibacterial activity of synthesized AgNPs against test bacterial pathogens.

Test	Zone of Inhibition (mm)				
Concentration (mM)/ Bacteria	MLE	1	2	5	10
E.coli	0	18.27± 1.37	19.55± 1.81	21.78± 1.51	22.09± 0.44
S.aureus	0	10.99± 0.42	9.11±0.28	9.18±0.18	9.95± 0.26

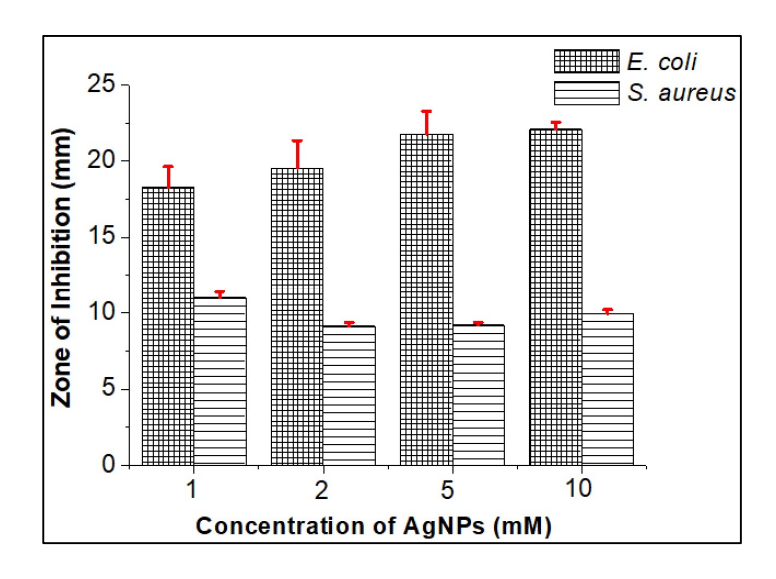


Figure 15. Antibacterial activity means the zone of inhibition (mm) of synthesized AgNPs against pathogenic bacterial strains

# Conclusion

AgNPs were successfully synthesized via biological method using MLE as a reducing agent and silver nitrate as the metal precursor. Phytochemical identification revealed that the MLE showed a high concentration of protein and carbohydrate as primary metabolites and the presence of flavonoids and sterols as secondary metabolites, which displayed dual performance of reducing agents, as well as capping agent/stabilizers. TEM images verified the formation of the well-dispersed and quasi-spherical shape of AgNPs with a size range between 8.25 nm and 19.34 nm with an average size of 12.60 nm  $\pm$  2.83 nm at the optimized

condition of 0.05 g/L (devoted as 100%) concentration of MLE, 2 mM of metal concentration, pH of 10 and 24 hr reaction time at room temperature. At optimized conditions, the AgNPs were highly crystalline in nature with FCC geometry, identified with XRD analysis. The stability of AgNPs synthesized at optimized conditions was confirmed by UV-vis spectral and zeta potential analysis. The synthesized AgNPs were seen to be as stable as when they were first made based on SPR peak in UV-Vis plot as well as did not show any precipitation or colour change in the colloidal AgNPs solution. The stability of synthesized AgNPs can be obtained by phytoconstituents in MLE coat these AgNPs or form an

organic matrix to embed them, thus preventing their aggregation and providing stability for a prolonged period of time. The zeta potential value of 23.61 mV also supports this conclusion. However, the stability of AgNPs decreased when the concentration of metal precursor increased. From the TEM image, the AgNPs were agglomerated when the concentration of AgNO<sub>3</sub> increased from 2 mM to 5 mM and 10 mM. Moreover, the Zeta potential values were decreased from 23.63 mV to 15.80 mV, and 9.75 mV as the stability of AgNPs decreased when 5 mM and 10 mM of initial concentration of metal precursors were used. The antibacterial study shows that the maximum zone of inhibition increases with increasing concentration of AgNPs where E. coli (Gram-negative) exhibited a higher zone of inhibition as compared to S. aureus (Gram-positive) with the value of maximum zone of inhibition around 18.27-22.09 mm for E. coli while S. aureus around 9.95-10.99 mm in diameter related to concentration bacteria of 30 µL. More extensive analysis is required for appropriate synthesis parameters and adequate concentration selection for use in biomedical applications and antibacterial control systems.

#### Acknowledgement

The authors acknowledge the materials, facilities, and financial support provided by University Teknologi MARA, Cawangan Pulau Pinang. This research was supported by the Malaysia Ministry of Higher Education – Fundamental Research Grant Scheme (FRGS/1/2019/STG01/UiTM/ 02/1) and (FRGS/1/2021/STG05/UiTM/02/9).

#### References

- 1. Royle, M., Bot, I., Mts, H. and Rafinesque, S. (2000). 8. Murdannia Royle, Ill. Bot. Himal. Mts. 1: 403. 1840, nom. cons. 5–12. Flora of China, 24: 25-31.
- Soraya, I., Sulaiman, C., Mohamad, A. and Ahmed, O. H. (2021). *Murdannia loriformis*: A review of ethnomedicinal uses, phytochemistry, pharmacology, contemporary application, and toxicology. *Evidence-Based Complementary and*

- Alternative Medicine (eCAM), 2021: 9976202.
- Poonthananiwatkul, B., Lim, R. H. M., Howard, R. L., Pibanpaknitee, P. and Williamson, E. M. (2015).
   Traditional medicine use by cancer patients in Thailand. *Journal of Ethnopharmacology*, 168: 100-107.
- 4. Jiratchariyakul, W. and Kummalue, T. (2011). Experimental therapeutics in breast cancer cells. Breast Cancer-Current and Alternative Therapeutic Modalities, 2011: 243-269.
- Kunnaja, P., Wongpalee, S. P., & Panthong, A. (2014). Evaluation of anti-inflammatory, analgesic, and antipyretic activities of the ethanol extract from *Murdannia loriformis* (Hassk.) Rolla Rao et Kammathy. *BioImpacts*, 4(4): 183-189.
- 6. Mohamad, N. N., Basir, M. R., Mahmood, A., Bakhari, N. A., Mydin, M. M., Arshad, N. M., Hamid, H. A., and Isa, N. (2022). Synthesis of silver nanoparticles using beijing grass extract as reducing agent and the comparative study of AgNPs toxicity. *International Journal Electroactive Materials*, 10: 1-11
- Mohamad, N. N., Mahmood, A., Bakhari, N. A., Mydin, M. M., Arshad, N. M. and Isa, N. (2021). Studies on surface plasmon resonance of Murdannia loriformis silver nanoparticles. Journal of Physics: Conference Series, 2129(1): 12084.
- 8. Azhar, A. S., Kamis, W. Z. W., Hamid, H. A., Kassim, N. F. A. and Isa, N. (2021). Removal of tartrazine dye using *Kyllinga Brevifolia* Extract and silver nanoparticles as catalysts. *Journal of Physics: Conference Series*, 2129(1): 12033.
- 9. Isa, N., Kian, T. W., Kawamura, G., Matsuda, A. and Lockman, Z. (2018). Synthesis of TiO<sub>2</sub> nanotubes decorated with ag nanoparticles (TNTs/AgNPs) for visible light degradation of methylene blue. *Journal of Physics: Conference Series*, 1082(1): 12105.
- Abdul Aziz, N. S., Isa, N., Osman, M. S., Wan Kamis, W. Z., So'aib, M. S. and Mohd Ariff, M. A. (2022). A mini review on the effects of synthesis conditions of bimetallic Ag/Si nanoparticles on their physicochemical properties. *International Journal of Nanoscience and Nanotechnology*, 18(4): 219-232.

- 11. Isa, N., Osman, M. S., Abdul Hamid, H., Inderan, V. and Lockman, Z. (2022). Studies of surface plasmon resonance of silver nanoparticles reduced by aqueous extract of shortleaf spikesedge and their catalytic activity. *International Journal of Phytoremediation*, 20:1-12.
- 12. Srikar, S. K., Giri, D. D., Pal, D. B., Mishra, P. K. and Upadhyay, S. N. (2016). Green synthesis of silver nanoparticles: a review. *Green and Sustainable Chemistry*, 6(1): 34-56.
- 13. Jamkhande, P. G., Ghule, N. W., Bamer, A. H. and Kalaskar, M. G. (2019). Metal nanoparticles synthesis: An overview on methods of preparation, advantages and disadvantages, and applications. *Journal of Drug Delivery Science and Technology*, 53: 101174.
- Isa, N., Wan Kamis, W. Z., Inderan, V., Husin, N. I., Ahmad, F. N., Bashirom, N. H. and Lockman, Z. (2019). Shape, size and dispersion of plant-driven silver nanoparticles for removal of methylene blue dyes. *Journal of Physics: Conference Series*, 1349(1): 012115.
- 15. Usman, H., Abdulrahman, F. I. and Usman, A. (2009). Qualitative phytochemical screening and in vitro antimicrobial effects of methanol stem bark extract of *Ficus thonningii* (Moraceae). *African Journal of Traditional, Complementary and Alternative Medicines*, 6(3): 289-295.
- Ministry of Health Malaysia. (2010). Guide to Nutrition Labelling and Claims (2010). Food Safety and Quality Division, Ministry of Health Malaysia, Putrajaya.
- Isa, N., Sarijo, S. H., Aziz, A. and Lockman, Z. (2017). Synthesis colloidal *Kyllinga brevifolia*-mediated silver nanoparticles at different temperature for methylene blue removal. In *AIP Conference Proceedings*, 1877(1): 070001.
- 18. Muniandy, S. S., Sasidharan, S. and Lee, H. L. (2019). Green synthesis of Ag nanoparticles and their performance towards antimicrobial properties.

- Sains Malaysiana, 48(4): 851-860.
- 19. Isa, N. and Lockman, Z. (2019). Methylene blue dye removal on silver nanoparticles reduced by *Kyllinga brevifolia*. *Environmental Science and Pollution Research*, 26(11): 11482-11495.
- Das, M. P., Livingstone, J. R., Veluswamy, P. and Das, J. (2018). Exploration of Wedelia chinensis leaf-assisted silver nanoparticles for antioxidant, antibacterial and in vitro cytotoxic applications. Journal of Food and Drug Analysis, 26(2): 917-925.
- 21. Abdelghaffar, F., Mahmoud, M. G., Asker, M. S. and Mohamed, S. S. (2021). Facile green silver nanoparticles synthesis to promote the antibacterial activity of cellulosic fabric. *Journal of Industrial and Engineering Chemistry*, 99: 224-234.
- 22. Mata, R., Nakkala, J. R. and Sadras, S. R. (2015). Biogenic silver nanoparticles from *Abutilon indicum*: their antioxidant, antibacterial and cytotoxic effects in vitro. *Colloids and Surfaces B: Biointerfaces*, 128: 276-286.
- 23. Yin, Y., Li, Z.-Y., Zhong, Z., Gates, B., Xia, Y. and Venkateswaran, S. (2002). Synthesis and characterization of stable aqueous dispersions of silver nanoparticles through the Tollens process. *Journal of Materials Chemistry*, 12(3): 522-527.
- 24. Stebounova, L. V, Guio, E. and Grassian, V. H. (2011). Silver nanoparticles in simulated biological media: a study of aggregation, sedimentation, and dissolution. *Journal of Nanoparticle Research*, 13(1): 233-244.
- 25. Sosa, Y. D., Rabelero, M., Treviño, M. E., Saade, H. and López, R. G. (2010). High-yield synthesis of silver nanoparticles by precipitation in a high-aqueous phase content reverse microemulsion. *Journal of Nanomaterials*, 2010: 392572.
- 26. Perugu, S., Nagati, V. and Bhanoori, M. (2016). Green synthesis of silver nanoparticles using leaf extract of medicinally potent plant Saraca indica: a novel study. *Applied Nanoscience*, 6(5): 747-753.